Adiabatic radio-frequency potentials for the coherent manipulation of matter waves

I. Lesanovsky,[1,*] T. Schumm,[1,2] S. Hofferberth,[1] L. M. Andersson,[1,3] P. Krüger,[1,4] and J. Schmiedmayer[1,†]
[1]*Physikalisches Institut, Universität Heidelberg, D-69120 Heidelberg, Germany*
[2]*Laboratoire Charles Fabry de l'Institut d'Optique, UMR 8105 du CNRS, F-91403 Orsay, France*
[3]*Department of Microelectronics and Information Technology, The Royal Institute of Technology, KTH, Electrum 229, SE-164 40, Kista, Sweden*
[4]*Laboratoire Kastler Brossel, 24 Rue Lhomond, 75005 Paris, France*
(Received 3 October 2005; revised manuscript received 19 January 2006; published 23 March 2006)

Adiabatic dressed state potentials are created when magnetic substates of trapped atoms are coupled by a radio-frequency field. We discuss their theoretical foundations and point out fundamental advantages over potentials purely based on static fields. The enhanced flexibility enables one to implement numerous configurations, including double wells, Mach-Zehnder, and Sagnac interferometers which even allows for internal state-dependent atom manipulation. These can be realized using simple and highly integrated wire geometries on atom chips.

DOI: 10.1103/PhysRevA.73.033619 PACS number(s): 03.75.Be, 32.80.Pj, 42.50.Vk

I. INTRODUCTION

Magnetic fields are powerful tools to control and manipulate the motion of neutral atoms [1,2]. These fields can either be created by (macroscopic) coils [3], free standing wires [4–6], or—as a result of the growing effort for miniaturization and integration—by surface-mounted microfabricated structures, so-called atom chips [7]. Compared to macroscopic setups, atom chips provide high magnetic field gradients [8] and therefore enable the realization of tightly confining traps. The flexibility of designing complex current and charge patterns on the chip allows for considerable freedom to engineer "potential landscapes" for neutral atoms. This has resulted in numerous designs of atom-optical elements such as traps, guides, beams splitters, and interferometers [9–13] with possible applications ranging from quantum information processing [14,15] to high precision measurements [16]. Even though many of these designs have been demonstrated experimentally [7,17,18], there have been enormous difficulties to realize a coherent beam splitter using microscopically tailored static or slowly varying fields [19].

Most of these difficulties stem from the fact that Maxwell's equations constrain the freedom to design static magnetic potentials. One consequence is that the number of potential minima created is less than or equal to the number of wires used [20]. Whereas regular strongly confining potential minima are created from quadrupole fields, the merging and splitting relies on higher order multipoles, usually the hexapole component, and thus results in a significantly weaker confinement. Consequently any dynamic splitting of a potential passes through a weakly confining region and creates an additional unwanted minimum, a loss channel. This splitting of two in two makes the central splitting region very unstable and therefore truly adiabatic manipulations are hard to perform [21].

These deficiencies can be overcome by using not only static fields but combining them with oscillating radio frequency (rf) or microwave near fields. The adiabatic dressed state potentials created in this way do not show the unwanted loss channels, keep the confinement tight during the splitting process, and consequently allow for a smooth transition from a single to two channels. Well controlled coherent splitting and simultaneous tight confinement of the atomic motion can be achieved even far away from the chip surface [22]. In addition adiabatic potentials permit the creation of nontrivial topologies like, for example, two-dimensional traps [23,24], closed path interferometers, and ring geometries. Also smooth transformations between different potential forms can be achieved.

In this paper we first discuss the theoretical foundations of the underlying coupling creating the adiabatic potentials and present their advantages. These are then applied to create basic atom optical elements such as a double well, a Mach-Zehnder interferometer, and a ring trap. We also outline the implementation of a state-dependent splitting scheme for atomic clouds.

II. THEORETICAL DESCRIPTION OF DRESSED rf POTENTIALS

We develop the theory by starting with the initial approach by Zobay and Garraway [23] and extending it to fully account for the vector properties of the magnetic fields involved. Only accounting for the latter leads to a complete description of the underlying couplings and the increased versatility of the resulting potentials.

We consider an alkali atom in a hyper-fine level designated by the quantum number F. Assuming that F remains a good quantum number even in the presence of a magnetic field, the atomic dynamics is governed by the Hamiltonian

$$H_{\text{initial}} = g_F \mu_B \mathbf{B}(\mathbf{r},t)\mathbf{F}. \tag{1}$$

Here g_F is the g factor of the hyper-fine level and $\mathbf{F}$ the angular momentum operator. We assume $\mathbf{B}(\mathbf{r},t)$ to consist of a static part $\mathbf{B}_S(\mathbf{r})$ and an oscillatory part of the form

*Electronic address: ilesanov@physi.uni-heidelberg.de
†Electronic address: schmiedmayer@atomchip.org

$$\mathbf{B}_O(\mathbf{r},t) = \mathbf{B}^A_{\mathrm{rf}}(\mathbf{r})\cos(\omega t) + \mathbf{B}^B_{\mathrm{rf}}(\mathbf{r})\cos(\omega t + \gamma). \tag{2}$$

As a first step we use the unitary transformation U_S to transform the Hamiltonian into a frame where the interaction of the atom with $\mathbf{B}_S(\mathbf{r})$ is diagonal, i.e.,

$$U_S^\dagger \mathbf{B}_S(\mathbf{r})\mathbf{F}U_S = [\mathfrak{R}_S \mathbf{B}_S(\mathbf{r})]\mathbf{F} = |\mathbf{B}_S(\mathbf{r})|F_z. \tag{3}$$

Here we have exploited that rotating the operator $\mathbf{F}$ by using U_S is equivalent to rotating the magnetic field vector $\mathbf{B}_S(\mathbf{r})$ by applying the appropriate rotation matrix $\mathfrak{R}_S$. The operator F_z can be represented as a diagonal matrix with the entries $-F \leqslant m_F \leqslant F$ and m_F denoting the magnetic hyper-fine sublevels. We proceed by applying another unitary operation $U_R = \exp\left[-i\frac{g_F}{|g_F|}F_z\omega t\right]$ which effectuates a transformation into a frame that rotates with the angular velocity ω around the local direction of the static field $\mathbf{e}_S = \frac{\mathbf{B}_S(\mathbf{r})}{|\mathbf{B}_S(\mathbf{r})|}$. The application of U_R leads to the emergence of additional terms that oscillate with the frequency 2ω. In the so-called rotating wave approximation—which we employ in the following—the oscillating terms are neglected. The now time-independent Hamiltonian reads

$$H = \left[g_F \mu_B |\mathbf{B}_S(\mathbf{r})| - \frac{g_F}{|g_F|}\hbar\,\omega \right] F_z + \frac{g_F \mu_B}{2} \begin{pmatrix} \bar{B}_x \\ \bar{B}_y \end{pmatrix}^T \begin{pmatrix} F_x \\ F_y \end{pmatrix}. \tag{4}$$

The term proportional to $\hbar\omega F_z$ arises from the transformation of the time derivative in the time-dependent Schrödinger equation. The field $\bar{\mathbf{B}}$ is given by

$$\bar{\mathbf{B}} = \mathfrak{R}_S \mathbf{B}^A_{\mathrm{rf}}(\mathbf{r}) + \mathfrak{R}_\delta \mathfrak{R}_S \mathbf{B}^B_{\mathrm{rf}}(\mathbf{r}), \tag{5}$$

where the matrix $\mathfrak{R}_\delta$ performs a rotation around the axis $\mathbf{e}_S$ by the angle

$$\delta = -\frac{g_F}{|g_F|}\gamma. \tag{6}$$

We want to emphasize that the sign of the rotation angle δ depends on the sign of the g factor. Therefore atoms in different hyperfine states will see different rf potentials even if they have the same magnetic moment $\mu = m_F \times g_F$.

The adiabatic potentials are the eigenvalues of the Hamiltonian (4)

$$V_{\mathrm{ad}}(\mathbf{r}) = m'_F \kappa \sqrt{\left[|\mathbf{B}_S(\mathbf{r})| - \frac{\hbar\omega}{|\kappa|} \right]^2 + \frac{1}{4}[\bar{B}_x^2 + \bar{B}_y^2]} \tag{7}$$

with $\kappa = g_F \mu_B$.

In the case of zero phase shift ($\gamma = 0$), i.e., a linear polarized rf field, the last term of the radical can be rewritten in a more convenient form: $\bar{B}_x^2 + \bar{B}_y^2 = \{\mathbf{e}_S \times [\mathbf{B}^A_{\mathrm{rf}}(\mathbf{r}) + \mathbf{B}^B_{\mathrm{rf}}(\mathbf{r})]\}^2$. Here it is immediately apparent that only the rf field components being perpendicular to the static field contribute.

III. REALIZATION OF ATOM OPTICAL ELEMENTS

A. Linear rf polarization—A double well

As a first example we consider the creation of a double-well potential starting from a Ioffe-Pritchard trap [7,31] which is one of the most commonly used trapping field configurations. Its magnetic field is given by

$$\mathbf{B}_S(\mathbf{r}) = G\rho[\cos\phi \mathbf{e}_x - \sin\phi \mathbf{e}_y] + B_{\mathrm{I}}\mathbf{e}_z. \tag{8}$$

Here G is the gradient of the quadrupole field and B_{I} the homogeneous Ioffe field strength. We superimpose a homogeneous oscillatory rf field perpendicular to the Ioffe field. Without loss of generality we take $\mathbf{B}^A_{\mathrm{rf}}(\mathbf{r}) = B_{\mathrm{rf}}\mathbf{e}_x$ and $\mathbf{B}^B_{\mathrm{rf}}(\mathbf{r}) = 0$. The unitary transformation which diagonalizes the static part of the Hamiltonian (1) is given by

$$U_S = \exp[iF_z\phi]\exp[iF_y\beta] \tag{9}$$

with $\cos\beta = \frac{B_{\mathrm{I}}}{|\mathbf{B}_S(\mathbf{r})|}$ and $\sin\beta = -\frac{G\rho}{|\mathbf{B}_S(\mathbf{r})|}$ and $|\mathbf{B}_S(\mathbf{r})| = \sqrt{G^2\rho^2 + B_{\mathrm{I}}^2}$. After the transformation into the rotated frame the adiabatic potential evaluates according to Eq. (7) to

$$V_{\mathrm{DW}}(\mathbf{r}) = m'_F \kappa \sqrt{\left[|\mathbf{B}_S(\mathbf{r})| - \frac{\hbar\omega}{|\kappa|} \right]^2 + \left[\frac{B_{\mathrm{rf}}}{2|\mathbf{B}_S(\mathbf{r})|} \right]^2 (B_{\mathrm{I}}^2 + G^2\rho^2\sin^2\phi)}. \tag{10}$$

Its minima are located at $\phi_1 = 0$ and $\phi_2 = \pi$. Assuming that $\rho \ll B_{\mathrm{I}}/G$ [37] we can approximate

$$V_{\mathrm{DW}}(\rho, \phi_{1,2}) = m'_F \kappa \sqrt{\frac{G^4}{B_{\mathrm{I}}^2}\left(\frac{\rho^2 - \rho_0^2}{2}\right)^2 + B_0^2} \tag{11}$$

with the position of the potential minimum

$$\rho_0 = \frac{1}{\sqrt{2}G}\sqrt{B_{\mathrm{rf}}^2 - B_{\mathrm{C}}^2}, \tag{12}$$

the potential bottom

$$m'_F \kappa B_0 = m'_F \kappa \frac{B_{\mathrm{rf}}}{4B_{\mathrm{I}}}\sqrt{4B_{\mathrm{I}}^2 + B_{\mathrm{C}}^2 - 2G^2\rho_0^2} \approx m'_F \kappa \frac{B_{\mathrm{rf}}}{2}\sqrt{1 + \frac{\hbar\Delta}{|\kappa|B_{\mathrm{I}}}}, \tag{13}$$

the critical field strength

$$B_{\mathrm{C}} = 2\sqrt{B_{\mathrm{I}}\frac{\hbar\Delta}{|\kappa|}} \tag{14}$$

and the detuning

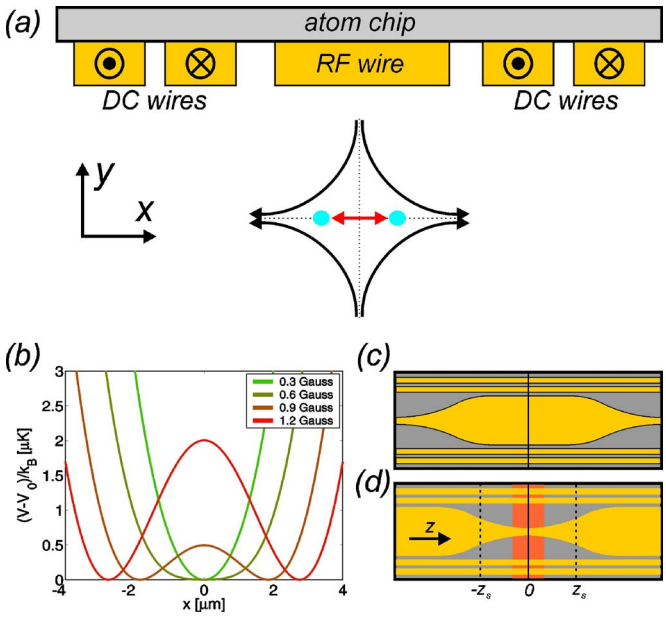

FIG. 1. (Color online) (a) Experimental realization of the double-well configuration. The quadrupole field is created by a surface-mounted dc four-wire structure. The rf field is generated by a central broad ac wire. Sufficiently close to the surface its rf field can considered to be homogeneous. (b) Depending on the actual rf field strength either a single- or a double-well is established. The potential bottom of the individual curves has been subtracted. (c),(d) Longitudinally modulating the shape of the rf wire results in a z-dependent variation of the rf amplitude. This can either be used to achieve a confinement along the longitudinal (z) axis (c) or a spatially dependent splitting which would result in an interferometer (d). Undesirable variations of the potential bottom can be, for example, compensated by placing a charged wire underneath the chip (red structure).

$$\hbar\Delta = \kappa B_{\mathrm{I}} - \hbar\omega. \tag{15}$$

In order to arrive at the last term of Eq. (13) we have exploited $G\rho_0 \ll B_{\mathrm{I}}$. For $B_{\mathrm{rf}} \leqslant B_{\mathrm{C}}$ the potential $V_{\mathrm{DW}}(\mathbf{r})$ exhibits only a single well whereas for $B_{\mathrm{rf}} > B_{\mathrm{C}}$ one encounters a double-well configuration [see Fig. 1(b)]. The trap frequency in each well evaluates approximately to

$$\omega_{\mathrm{T,rf}} = \sqrt{\frac{m'_F \kappa}{mB_0}} \frac{G^2 \rho_0}{B_{\mathrm{I}}} \tag{16}$$

with m being the mass of the atom considered.

There are several advantages of a rf interferometer over a static two-wire configuration [11,25,26]:

(1) The capability of performing a smooth transition from a true single well to a double well, by varying any of the parameters Δ, B_{rf}, and B_{I}. In contrast, in the static case one encounters a transition from two vertically to two horizontally split minima, if the strength of a homogeneous bias field is modulated [11]. In the vicinity of the splitting region this leads to unwanted tunneling processes into the second vertical (loss) channel just before the intended splitting sets in [25]. This poses a severe obstacle for establishing an adiabatic process. In addition the rf realization of the double well conserves the parabolic confinement perpendicular to the splitting direction even in the vicinity of the splitting region. Here the confinement in the static configuration in both directions relies solely on a quartic potential.

(2) In the static realization the distance between the potential minima scales according to $\rho_0 \propto \sqrt{b}$. Here b is the strength of a homogenous magnetic field which eventually gives rise to the splitting of the hexapole into two quadrupole minima [21]. However, in order to have a stable splitting distance one has to precisely control the field strength b, i.e., keep its fluctuations Δb small. This is extremely hard in the vicinity of $b=0$ since $\Delta\rho_0/\Delta b \propto b^{-1/2}$. Unlike this the splitting distance in the rf case obeys $\rho_0 \propto B_{\mathrm{rf}}$ (for zero detuning). Thus we find ρ_0 to be much less sensitive with respect to fluctuations in B_{rf} particularly if B_{rf} is small.

(3) The rf adiabatic potential keeps much tighter confining wells even far away from the field generating structures, i.e., the chip surface. This can be illustrated considering an atom chip with structure size d. For the sake of simplicity the quadrupole for the rf setup shall be created by a sideguide configuration [7] in a distance d above the chip surface. The static implementation of the double well consists of two wires separated by $2d$ [21]. Provided that the wire current I and B_{I} are equal for both setups and assuming for simplicity $\Delta=0$ the trap frequencies and the height of the barrier between the wells obey

$$\frac{\omega_{\mathrm{T,rf}}}{\omega_{\mathrm{T,static}}} \propto \frac{d}{\rho_0}\sqrt{\frac{B_{\mathrm{rf}}}{B_{\mathrm{I}}}}, \tag{17}$$

$$\frac{h_{\mathrm{T,rf}}}{h_{\mathrm{T,static}}} \propto d^2 \frac{G^2}{B_0 B_I}. \tag{18}$$

The essence of these expressions is their scaling with respect to the parameter d which refers not only to the structure size but also to the distance of the potential wells to the chip surface. Compared to the static two-wire case, a similar rf trap allows for realizing the same confinement with larger structures and thus farther away from the chip surface. The latter is of particular importance as hereby coherence-destroying surface interactions [27,28] are strongly inhibited. The stronger increase of the potential barrier in the rf case is advantageous as it permits a true spatial separation of trapped atom clouds even for small splitting distances.

The potential of the rf technique to coherently control the motion of atoms has recently enabled the demonstration of coherent splitting of a Bose-Einstein condensate (BEC) on an atom chip [22].

In Fig. 1(a) we present how a highly integrated realization of a rf double well could look like. The quadrupole field is generated by a four-wire structure carrying counter-propagating dc currents. In between these wires there is a broad wire flown through by an ac current. Sufficiently close to this wire, the resultant rf field can be considered to be homogeneous. The Ioffe field pointing into the plane of view is generated by additional wires which are not shown here [7]. The potential bottom of the rf double well increases proportional to $(B_{\mathrm{rf}}-B_{\mathrm{C}})^2$. This provides a convenient mechanism to achieve confinement in the longitudinal direction. A

z dependence of the rf amplitude, i.e., $B_{\rm rf}=B_{\rm rf}(z)$, can be achieved by shaping the rf wire [30]. For example, a wire geometry creating a symmetric increase of the current density around $z=0$, consequently, will lead to a symmetric increase of the rf amplitude [see Fig. 1(c)]. Hence, depending on the actual value of $B_{\rm rf}$ a three-dimensionally confining single or double well is achieved. Similarly a Mach-Zehnder interferometer can be realized by varying the rf amplitude such that $B_{\rm rf}(0)>B_{\rm C}$ and $B_{\rm rf}(z)|_{|z|\geqslant z_S}<B_{\rm C}$ with z_S defining the length of the splitting region as indicated in Fig. 1(d). The variations of the potential bottom can be compensated by applying either a spatially varying Ioffe field or an additional external potential. The latter can be realized for instance by placing a charged wire underneath the chip [29]. The corresponding electric potential reads $U_{\rm el}(\mathbf{r})=-\frac{\alpha}{2}|\mathbf{E}(\mathbf{r})|^2$ [7].

B. Arbitrary rf polarization—A ring interferometer

As a second example we construct a more complex trapping geometry by employing two phase-shifted rf fields. We consider two orthogonal rf fields of the form $\mathbf{B}_{\rm rf}^A(\mathbf{r})=\frac{B_{\rm rf}}{\sqrt{2}}\mathbf{e}_x$ and $\mathbf{B}_{\rm rf}^B(\mathbf{r})=\frac{B_{\rm rf}}{\sqrt{2}}\mathbf{e}_y$, which are superimposed on the static $\mathbf{B}_S(\mathbf{r})$. According to Eq. (7) the corresponding adiabatic potential evaluates to

$$V_{\rm R}(\mathbf{r})=m_F'\kappa\sqrt{\left[|\mathbf{B}_S(\mathbf{r})|-\frac{\hbar\omega}{|\kappa|}\right]^2+\frac{B_{\rm rf}^2}{8|\mathbf{B}_S(\mathbf{r})|^2}\{G^2\rho^2[1+\sin(2\phi)\cos\,\delta]+2B_{\rm I}[B_{\rm I}+|\mathbf{B}_S(\mathbf{r})|\sin\,\delta]\}}. \tag{19}$$

For $\cos\,\delta>0$ we find the minima and maxima of the potential at $\phi_{\rm min}=\frac{3}{4}\pi,\frac{7}{4}\pi$ and $\phi_{\rm max}=\frac{1}{4}\pi,\frac{5}{4}\pi$, respectively. If $\cos\,\delta<0$ the positions of the minima and maxima simply swap. Assuming $\rho\ll B_{\rm I}/G$ the radial position of these extrema is

$$\rho_0=\frac{1}{2G}\sqrt{B_{\rm rf}^2[1-\cos\,\delta\sin(2\phi)+\sin\,\delta]-2B_{\rm C}^2}. \tag{20}$$

Hence for $\cos\,\delta>0$ and $B_{\rm rf}<\sqrt{\frac{2}{1+\cos\,\delta+\sin\,\delta}}B_{\rm C}$ or $\cos\,\delta<0$ and $B_{\rm rf}<\sqrt{\frac{2}{1-\cos\,\delta+\sin\,\delta}}B_{\rm C}$ solely a single minimum can be achieved. For $\delta=\frac{3}{2}\pi$ in any case only a single minimum is found.

In Fig. 2(a) we present how such a setup can be realized in a highly integrated way. The static quadrupole field is generated by a three wire setup. The two outer wires also serve as rf sources that are positioned such that two orthogonally polarized homogeneous fields in the vicinity of the quadrupole are created.

The versatility of the potential (19) lies in the fact that by simply varying the phase shift δ, i.e., changing the polarization of the rf field, one can either accomplish a single well, a double well, or a ring configuration. Even a rotating double well is achievable by appropriately tuning the phase and the rf amplitude. The double-well configuration with the strongest confinement is achieved for $\gamma=0$, i.e., vanishing relative phase shift of the rf fields. Increasing the phase shift from $\delta=0$ to $\delta=\frac{\pi}{2}$, i.e., from linear to circular polarization, results in a smooth transition to a ring-shaped potential of adjustable radius. This transition is shown in Fig. 2(b). The potentials shown are calculated for the typical set of experimental parameters $B_{\rm I}=1$ G, $G=0.2$ G/μm, $B_{\rm rf}=1.3$ G, and $\omega=2\pi\times1.26$ MHz. In order to generate a confinement also in the longitudinal (z) direction we impose a modulation of the rf amplitude of the form $B_{\rm rf}(z)=(B_{\rm rf}+G_{\rm rf}^2z^2)$. In Fig. 2(c) the $m_Fg_FE=k_B\times1.1$ μK isosurface for $G_{\rm rf}^2=0.05$ G/m^2 is depicted. The ring-shaped potential is thus capable of confining BECs as the typical energy scale associated to such matter waves is in the nano-Kelvin regime.

The setup allows one to examine the collective ground state of ultracold atoms trapped on a ring [32]. Also building a ring interferometer (Sagnac interferometer) for matter waves is possible. Coherence preserving loading of the latter could be done by preparing an ultra-cold atomic ensemble in the static wire trap. Switching on the rf fields thereafter, and establishing the appropriate phase shift δ leads to a well-controlled transition to the ring-shaped potential. Such traps are particularly suited for building gyroscopes or rotation sensors. Gupta *et al.* [33] have recently succeeded in loading

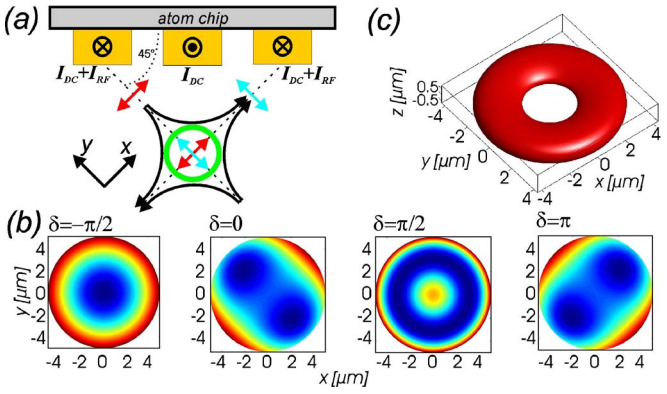

FIG. 2. (Color online) (a) Experimental setup for realizing a ring-shaped potential. The static quadrupole field is generated by a three wire configuration. The two outer wires also carry rf currents which generate two phase shifted and orthogonally polarized oscillating homogeneous fields in the vicinity of the quadrupole center. (b) Depending on the phase shift δ either a single well, a double-well, or a ring-shaped potential emerge. (c) A 3D confinement is achieved by introducing a spatially dependent rf amplitude of the form $B_{\rm rf}(z)=1.3$ G$+0.05$ (G/m^2)z^2. Visualization of the $m_Fg_FE=k_B\times1.1$ μK isosurface for this case.

a ring-shaped waveguide with a BEC. Their setup consists of millimeter-sized coils forming a magnetic quadrupole ring with diameters ranging from 1.2 to 3 mm. However, generating BECs which are phase coherent over the entire ring is extremely difficult in such a macroscopic trap. In order to avoid the necessity of cooling to extremely low temperatures it is beneficial to use small rings with diameters of a few micrometers.

Also internal state-dependent manipulation of atoms can be achieved by using the potential (19). Let us consider for instance the two hyperfine states $|1\rangle$ and $|2\rangle$ with the same magnetic moment $\mu=m_F g_F \mu_B$. Consequently in a static field atoms in either of these states are subjected to the same trapping potential. Suppose now the rf field is switched on adiabatically such that $m'_F=m_F$. In the case when $g_{F|1\rangle}=-g_{F|2\rangle}$ we have $\delta_{|1\rangle}=-\delta_{|2\rangle}$. Thus for $\delta_{|1\rangle}=\frac{\pi}{2}$ atoms being in state $|1\rangle$ see a ring whereas atoms in state $|2\rangle$ are confined to a single centered potential minimum as seen in Fig. 2(b).

IV. CONCLUSION

In conclusion dressed rf adiabatic potentials are versatilely applicable to build atom optical elements and offer a number of significant advantages over their static implementations. Radio frequency-based traps provide tight confinement even at large surface distances and allow for a smooth transition from a single to a double well. Moreover, a rf double well is more robust against experimental fluctuations against its static counterpart which is certainly advantageous for performing tunneling experiments. This technique paves the way to the realization of complex coherence preserving potentials on a microscale by using simple and highly integrated setups. This is of particular importance for such demanding applications as quantum information processing and high precision measurements based on matter wave interference.

After submission of this manuscript several other works discussing applications of rf potentials has been published [34–36,38].

ACKNOWLEDGMENTS

We acknowledge financial support from the European Union, Contracts No. IST-2001-38863 (ACQP), No. MRTN-CT-2003-505032 (Atom Chips), No. HPMF-CT-2002-02022, the Deutsche Forschungsgemeinschaft, Contract No. SCHM 1599/1-1, and the German Federal Ministry of Education and Research (BMBF) through the German-Israel Project DIP-F 2.2. P.K. acknowledges support from the Alexander von Humboldt Foundation and the EU (Marie Curie program).

[1] A. L. Migdall, J. V. Prodan, W. D. Phillips, T. H. Bergeman, and H. J. Metcalf, Phys. Rev. Lett. **54**, 2596 (1985).
[2] C. E. Wieman, D. E. Pritchard, and D. J. Wineland, Rev. Mod. Phys. **71**, S253 (1999).
[3] T. Bergeman, G. Erez, and H. J. Metcalf, Phys. Rev. A **35**, 1535 (1987).
[4] J. Schmiedmayer, Phys. Rev. A **52**, R13 (1995).
[5] J. Fortagh and A. Grossman, Phys. Rev. Lett. **81**, 5310 (1998).
[6] J. Denschlag, D. Cassettari, and Jörg Schmiedmayer, Phys. Rev. Lett. **82**, 2014 (1999).
[7] R. Folman *et al.*, Adv. At., Mol., Opt. Phys. **48**, 263 (2002).
[8] J. Reichel and J. H. Thywissen, J. Phys. IV **116**, 265 (2004).
[9] D. Cassettari, B. Hessmo, R. Folman, T. Maier, and J. Schmiedmayer, Phys. Rev. Lett. **85**, 5483 (2000).
[10] D. Muller *et al.*, Opt. Lett. **25**, 1382 (2000).
[11] E. A. Hinds, C. J. Vale, and M. G. Boshier, Phys. Rev. Lett. **86**, 1462 (2001).
[12] W. Hänsel, J. Reichel, P. Hommelhoff, and T. W. Hänsch, Phys. Rev. A **64**, 063607 (2001).
[13] E. Andersson, T. Calarco, R. Folman, M. Andersson, B. Hessmo, and J. Schmiedmayer, Phys. Rev. Lett. **88**, 100401 (2002).
[14] T. Calarco, E. A. Hinds, D. Jaksch, J. Schmiedmayer, J. I. Cirac, and P. Zoller, Phys. Rev. A **61**, 022304 (2000).
[15] M. A. Cirone *et al.*, Eur. Phys. J. D **35**, 165 (2005).
[16] M. Kasevich and S. Chu, Phys. Rev. Lett. **67**, 181 (1991).
[17] P. Hommelhoff *et al.*, New J. Phys. **7**, 3 (2005).
[18] A. Günther, M. Kemmler, S. Kraft, C. J. Vale, C. Zimmerman, and J. Fortagh, Phys. Rev. A **71**, 063619 (2005).
[19] Y. Shin, C. Sanner, G. B. Jo, T. A. Pasquini, M. Saba, W. Ketterle, D. E. Pritchard, M. Vengalattore, and M. Prentiss, Phys. Rev. A **72**, 021604(R) (2005).
[20] T. J. Davis, Eur. Phys. J. D **35**, 165 (2005).
[21] J. Estève *et al.*, Eur. Phys. J. D **35**, 141 (2005).
[22] T. Schumm *et al.*, Nat. Phys. **1**, 57 (2005).
[23] O. Zobay and B. M. Garraway, Phys. Rev. Lett. **86**, 1195 (2001); Phys. Rev. A **69**, 023605 (2004).
[24] Y. Colombe *et al.*, Europhys. Lett. **67**, 593 (2004).
[25] J. A. Stickney and A. A. Zozulya, Phys. Rev. A **68**, 013611 (2003).
[26] J. Denschlag *et al.*, Appl. Phys. B **69**, 291 (1999).
[27] C. Henkel, P. Krüger, R. Folman, and J. Schmiedmayer, Appl. Phys. B **76**, 173 (2003).
[28] C. Schroll, W. Belzig, and C. Bruder, Phys. Rev. A **68**, 043618 (2003).
[29] P. Kruger, X. Luo, M. W. Klein, K. Brugger, A. Haase, S. Wildermuth, S. Groth, I. Bar-Joseph, R. Folman, and J. Schmiedmayer, Phys. Rev. Lett. **91**, 233201 (2003).
[30] S. Kraft *et al.*, Eur. Phys. J. D **35**, 119 (2005).
[31] D. E. Pritchard *et al.*, Phys. Rev. Lett. **51**, 1336 (1983).
[32] O. E. Alon *et al.*, Europhys. Lett. **67**, 8 (2004).
[33] S. Gupta, K. W. Murch, K. L. Moore, T. P. Purdy, and D. M. Stanper-Kurn, Phys. Rev. Lett. **95**, 143201 (2005).
[34] T. Fernholz *et al.*, e-print physics/0512017.
[35] Ph. W. Courteille B. Deh, J. Fortagh, A. Günther, S. Kraft, C. Marzok, S. Slama, and C. Zimmerman, J. Phys. B **39**, 1055 (2006).
[36] O. Morizot *et al.*, e-print physics/0512015.
[37] The validity of this condition can be assured by applying a sufficiently large Ioffe field.
[38] G. A. Kouzaev and K. J. Sand, e-print cond-mat/0602210.